Preparation of $Pb(Zr_{0.52}Ti_{0.48})O_3$ thin films on silicon-on-insulator substrates by excimer laser deposition combined with rapid thermal annealing

LIRONG ZHENG, CHENGLU LIN, SHICHANG ZOU
State Key Laboratory of Functional Materials for Informatics, Shanghai Institute of Metallurgy, Chinese Academy of Sciences, 865 Changning Road, Shanghai 200050, People's Republic of China

In this paper we report the fabrication of ferroelectric $Pb(Zr_{0.52}Ti_{0.48})O_3$ (PZT) thin films on Si-on-Insulator (SOI) substrates with and without an electrode by pulsed excimer laser deposition combined with rapid thermal annealing. Based on the structural and interfacial characteristics analysis by X-ray diffraction (XRD), Rutherford backscattering spectroscopy (RBS), cross-sectional transmission electron microscopy (XTEM) and automatic spreading resistance measurement (ASR), the film structure and orientation were revealed to be dependent on the annealing time and annealing temperature as well as deposition temperature. From RBS spectra and XTEM observation it is shown that the PZT thin films did not interact with the top silicon layers of SOI and that the composition of the film was similar to the target. The ASR measurements showed that the electrical properties of PZT/SOI as well as PZT/Pt/SOI were abrupt, and that the electrical properties of the SOI substrates were still good after the PZT growth.

1. Introduction

Ferroelectric thin films are of considerable interest for use in nonvolatile random access memories (RAMs). One of the principal advantages of such devices is their high degree of radiation hardness [1,2]. A raw memory array of ferroelectric cells will typically withstand a $>5\times10^6$ rad cm^{-2} total dose of 1-MeV gammas, $>10^{11}$ rad cm^{-2} s dose rate, 10^{14} neutrons per cm^2, and exhibit not as much as a single event upset. As a result, such ferroelectric memories are potentially attractive for both military systems and in civilian satellite applications. In order to increase the reliability of these devices when working under extreme conditions, a radiation-hardened substrate is often used. Silicon-on-insulator (SOI) technology has been shown to have significant performance and fabrication advantages over conventional bulk processing for a wide variety of large scale Integrated Circuit applications. Advantages in radiation environments has generated significant additional interest in this technology from the military and space science communities [3,4]. The combination of this technology with ferroelectric capacitors produces extreme hard RAMs.

There has been a lot of work performed on the fabrication of ferroelectric PZT thin films on bulk silicon and platinum substrates [5, 6]. A SOI structure with a $BaTiO_3$ buried insulator has been investigated by Yamanashi *et al.* [7]. In this paper, we report the fabrication of PZT thin films on SOI by the combination of laser deposition and rapid thermal annealing. Although there are considerable similarities between the use of SOI or bulk silicon substrates, the fabrication of a PZT thin film or a PZT capacitor on SOI substrates is highly desirable and the combination of laser deposition and rapid thermal annealing (RTA) offers an interesting route to the production of such structures.

2. Experimental procedure

SOI substrates were formed by ion beam synthesis. Device grade *p*-type silicon wafers of $\langle100\rangle$ orientation were implanted with 170 keV oxygen ions to a dose of 1.5×10^{18} cm^{-2}. During implantation, the wafers were maintained at 680 °C. After implantation, the wafers were annealed at 1300 °C for 5 h in an Ar + 0.5 % O_2 ambient. Planar SOI structures with abrupt interfaces were formed [8], consisting of an overlayer of 250 nm single crystal silicon and a buried stoichiometric SiO_2 layer 370 nm thick.

0022–2461 © 1996 Chapman & Hall

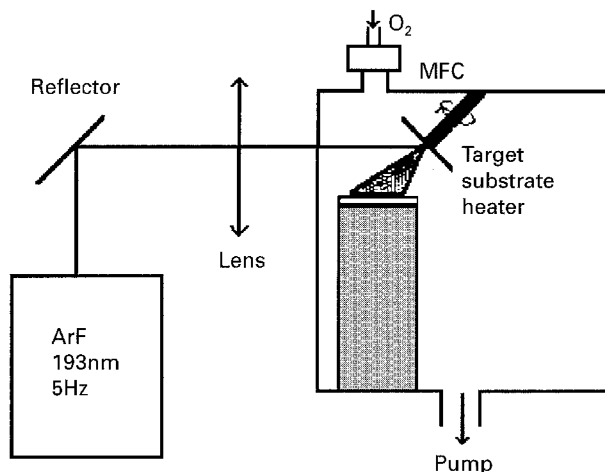

Figure 1 Schematic diagram of the pulsed laser deposition setup.

The PZT ceramic target, which was sintered at high temperature after standard ceramic powder processing, was near the morphotropic phase boundary composition ($PbZr_{0.52}Ti_{0.48}O_3$) with a few per cent excess lead oxide. The perovskite structure of the target was confirmed by X-ray diffraction. The target was polished before each deposition.

PZT thin films on SOI were fabricated by a pulsed excimer laser (Lambda Physik, LPX120icc) deposition system. A schematic diagram of this deposition setup is presented in Fig. 1. The frequency and wavelength of the ArF excimer laser were set to 5 Hz and 193 nm, the energy and pulse width were 120 mJ and 10 ns respectively. Followed by a total-reflector, the beam was focused by a UV grade plano-convex lens of 50 cm focal length and then brought into the quartz chamber and was incident onto the rotating target at an angle of 45°. The stability and loss of the beam energy before impinging on the target were measured by an energy meter. The energy fluence of the laser beam was about $4\,J\,cm^{-2}$.

SOI substrates were placed horizontally at a distance of 5 cm from the ablated spot. During deposition, a 100% O_2 ambient was maintained by a mass flow controller (MFC) at a flow of $25\,cm^3$ per min, and at a uniform pressure of 13.3 Pa. The films thus deposited at 200–700 °C were rapid thermally annealed in flowing oxygen at 600–750 °C for different times. The heating processes can be divided into three steps. First, from room temperature to 200 °C with heating rate of 600 °C per min, then from 200 °C to a final annealing temperature with heating rate 2700 °C per min, and finally, a soak at this final temperature for times ranging from 10 s to 30 min. The films were cooled slowly (less than 40 °C per min) in the vicinity (430–300 °C) of the phase transition.

3. Results & Discussion
3.1. Structure
3.1.1. Annealing time dependence
The crystallographic structure of the films was investigated by X-ray diffraction (XRD) using $CuK_\alpha(\lambda = 10.541\,nm)$ at room temperature. Fig. 2 (a–d) shows the XRD patterns for the films deposited at 400 °C on

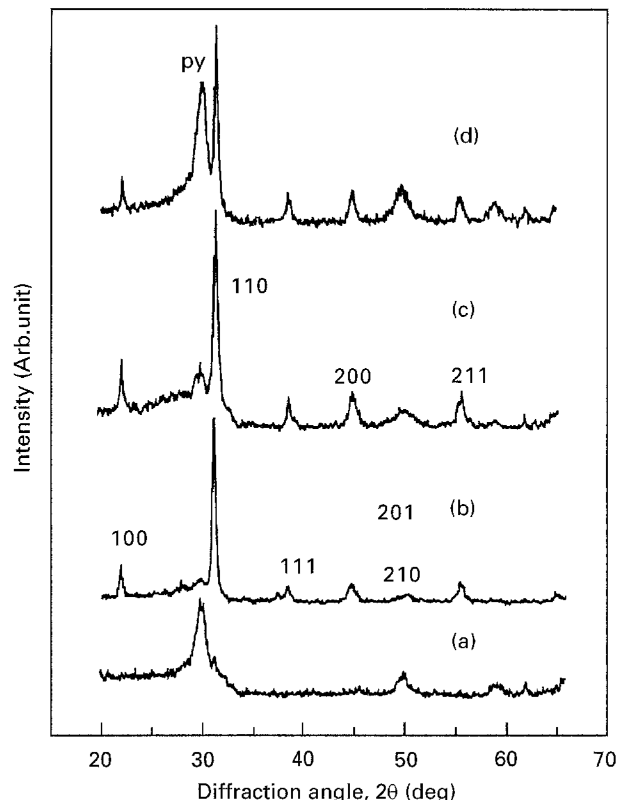

Figure 2 XRD patterns for PZT thin films deposited on SOI substrates and annealed at 650 °C for (a) 60 s, (b) 120 s, (c) 180 s and (d) 300 s. (py: pyrochlore, 100, 110 etc.: plane of perovskite).

SOI and subsequently annealed at 650 °C for various times, the crystallographic properties of the deposited films were strongly dependent upon the annealing time. The films were amorphous for as-deposited material, and was dominantly the pyrochlore phase (which does not show ferroelectricity and has its main diffraction peak at $2\theta = 29.6°$) for annealing times less than 100 s or more than 300 s. Only within the operational window of annealing time between 120–180 s, did the PZT films crystallize into a single perovskite phase. It should be noted that this required annealing time is much shorter than that for PZT on bulk silicon, which is about 7 min under the same conditions as was reported previously [9, 10]. This result means that PZT films are more easily crystallized on SOI substrates than on bulk silicon. The reason for this behaviour may be attributed to the surface structure of SOI. In the top silicon layer of our ion beam synthesized SOI, there are more dislocations and interstitial oxygen atoms than in bulk silicon and these dislocations may act as nucleation sites and in addition the interstitial oxygen atoms may increase the probability of Pb incorporation into the film.

Fig. 3(a–d) shows the XRD patterns for the films deposited at 400 °C on Pt-coated SOI substrates and annealed at 650 °C for various times. With a Pt electrode as a buffer layer, the results were very similar to those of PZT deposited on Pt/Si we reported in reference [10]. The pure single phase perovskite structured PZT films were obtained within annealing times between 180–360 s, with mainly ⟨110⟩ and

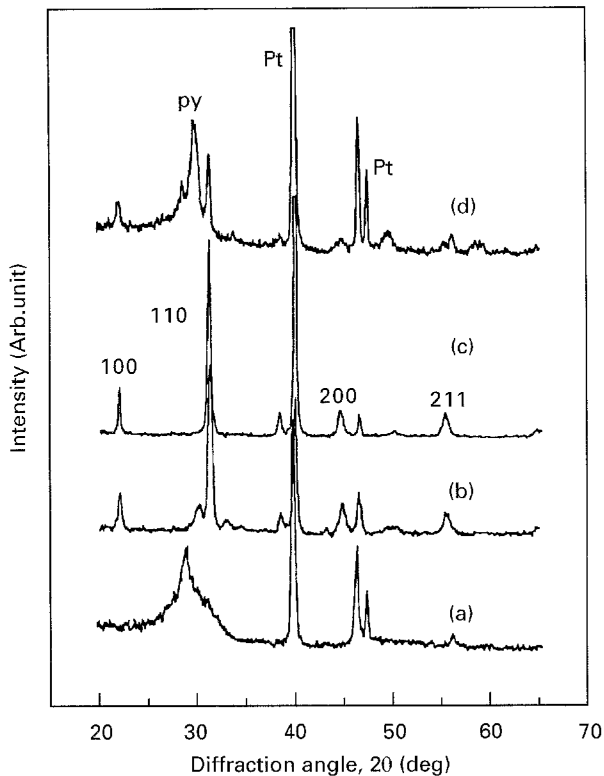

Figure 3 XRD patterns for PZT thin films deposited at 400 °C on Pt-coated SOI substrates and annealed at 650 °C for (a) 0 s, (b) 180 s, (c) 200 s and (d) 420 s. (py: pyrochlore, 100, 110 etc.: plane of perovskite).

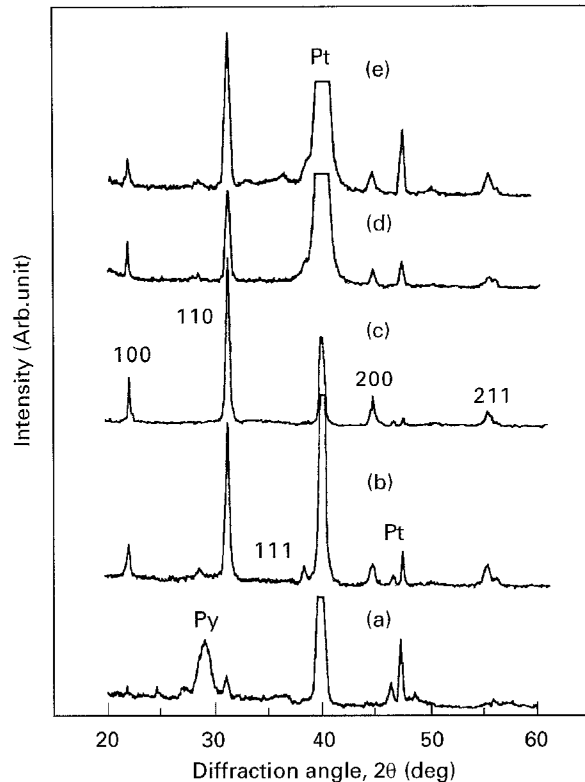

Figure 4 XRD patterns for PZT thin films deposited at 400 °C and annealed at (a) 550 °C for 500 s, (b) 600 °C for 290 s, (c) 650 °C for 200 s, (d) 700 °C for 30 s and (e) 750 °C for 10 s. (py: pyrochlore, 100, 110 etc.: plane of perovskite).

⟨100⟩ orientations. However, any further increase in the annealing time to beyond 360 s leads to an increase in the pyrochlore phase content of the films.

3.1.2. Annealing temperature dependence

The influence of annealing temperature on the formation of the perovskite structure is shown in Fig. 4(a–e) where the films were deposited at 400 °C on Pt/SOI. The results of PZT grown directly on SOI were similar. In our experiments, however, an annealing temperature less than about 525 °C is unable to crystallize PZT into the perovskite structure regardless of the length of the annealing time. When the film was annealed at 550 °C, a perovskite diffraction peak first appeared after annealing for 15 min. When it was annealed at 600 °C, more than 290 s of annealing time was required for the formation of a pure single phase perovskite film. However, when annealed at 750 °C for 10 s, the film was observed to be pure perovskite. The required annealing time for the formation of a pure single phase perovskite film decreases when the annealing temperature increases. From Fig. 4, we also find that the preferred orientation in the ⟨110⟩ direction of the films is almost independent on the annealing temperature.

3.1.3. Deposition temperature dependence

Fig. 5(a–f) shows the dependence of crystalline structure on the deposition temperature. The PZT films were deposited at 450, 550 and 700 °C, then they were

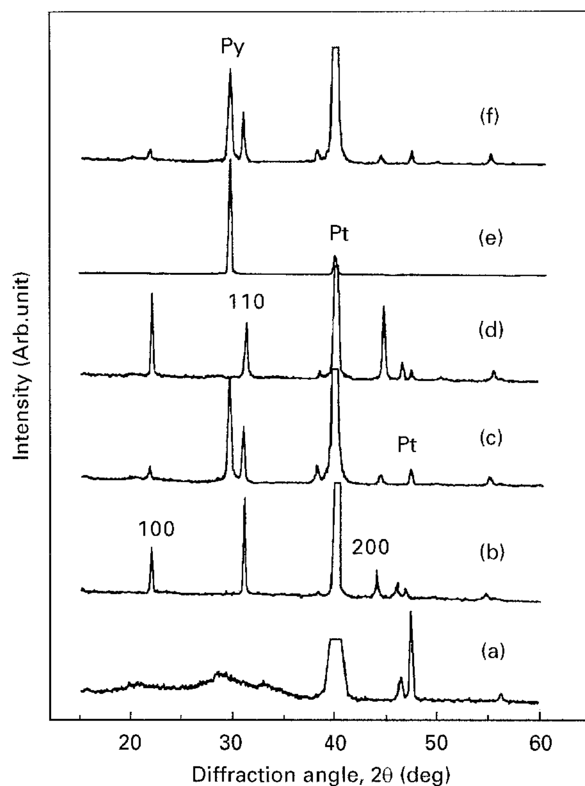

Figure 5 XRD patterns for PZT films deposited at different temperatures and annealed by RTA. (a) 450 °C as deposited, (b) 450 °C deposited and annealed at 750 °C for 100 s, (c) 550 °C as-deposited, (d) 550 °C deposited and annealed at 750 °C for 100 s (e) 700 °C as-deposited, (f) 700 °C deposited and annealed at 750 °C for 100 s.

annealed at 750 °C for 100 s. As we see, the 450 °C as-deposited film was amorphous, the 550 °C as-deposited film was a mixture of pyrochlore and perovskite phase and the 700 °C as-deposited film was pure pyrochlore phase. After a 750 °C 100 s annealing, the 450 and 550 °C deposited films as well as lower temperature deposited films (<450 °C) were crystallized into a pure perovskite structured single phase, but the higher temperature deposited films such as that deposited at 700 °C were no longer crystallized into pure perovskite phase as is shown in Fig. 5f. This may be due to the volatility of Pb during the high temperature deposition. This result suggests that a reduction of the deposition temperature enables as-deposited films to crystallize into pure perovskite structured single phase films. However, we find that a higher temperature deposition developed a ⟨100⟩ preferred orientation after annealing as is shown in the increase of the ⟨100⟩ orientation in Fig. 5(d).

3.2. Microstructure

The microstructure of PZT films deposited on SOI and Pt-coated SOI substrates were examined by cross-sectional transmission electronic microscopy (XTEM) and showed sharp interfaces and dense films. Fig. 6 (a and b) shows XTEM results for a sample deposited at 400 °C and annealed at 650 °C. The multilayer structure can be clearly observed. The interfaces between PZT and the top silicon layer as well as Pt were very sharp and the PZT films were very dense. From the thickness of the PZT layer, we estimated a deposition rate of about 0.2 nm per shot.

3.3. Interface and composition

Rutherford backscattering spectroscopy (RBS) analysis of the interfaces and the stiochiometry of the PZT films on SOI or Pt/SOI also revealed sharp interfaces of PZT–SOI, PZT–Pt/SOI, and a Zr:Ti ratio of 52:48 and a Pb/(Zr + Ti) ratio of 1. Fig. 7a is an RBS spectrum of a PZT/SOI sample deposited at 400 °C and annealed at 650 °C for 120 s. As expected, the film composition was calculated to be Zr:Ti = 52:48 and Pb/(Zr + Ti) = 1. The position of the silicon channel step at channel 145 clearly suggests that the annealed PZT film did not interact with the top silicon layer of the SOI substrate. The interface between PZT on SOI was found to be better than that we reported for PZT on silicon [9]. This may be due to the reduction of annealing time of PZT on SOI, as we discussed in the previous section, the annealing time is only 120 s for PZT on SOI whilst about 7 min is required for PZT on silicon. Thus, interdiffusion between PZT and SOI can be more easily controlled by rapid thermal annealing as compared to PZT on silicon due to its shorter heating time. In addition, the rapid thermal annealing of PZT films at 650 °C for 120 s did not affect the SOI substrate, as is indicated by a comparison with the RBS spectra of an SOI substrate before deposition, see Fig. 7b.

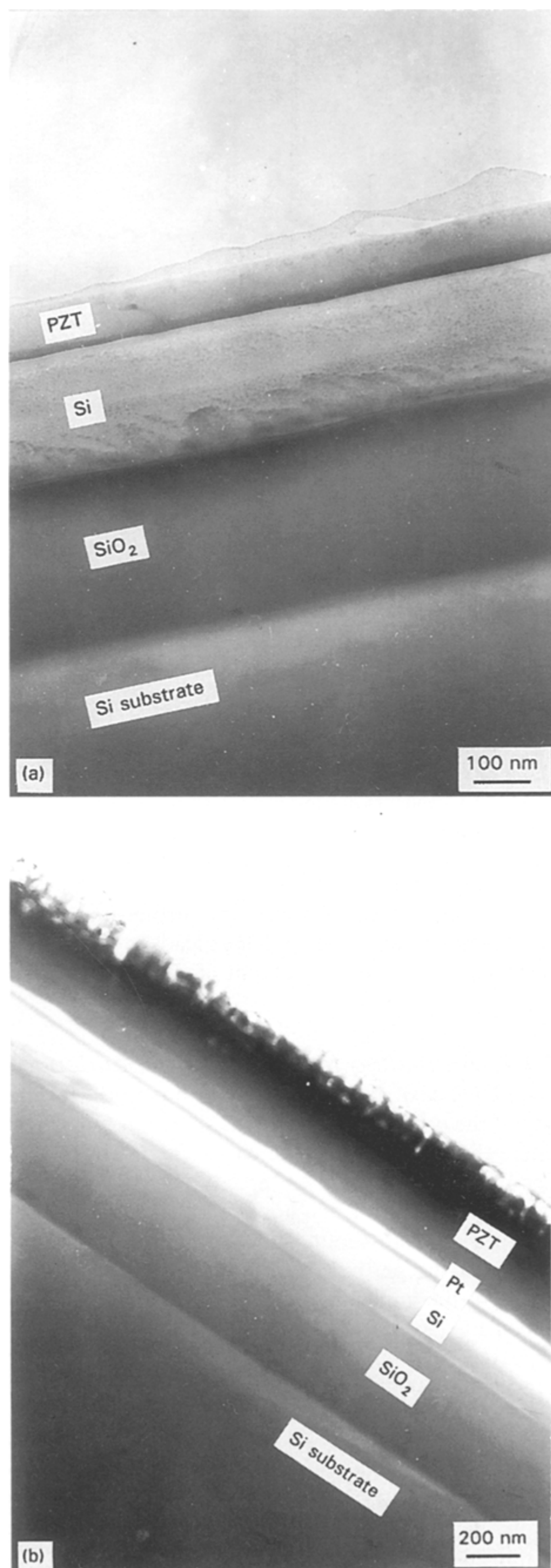

Figure 6 Cross-sectional TEM micrograph from (a) PZT on SOI substrates and (b) PZT on Pt-coated SOI substrates.

3.4. Electrical properties

Fig. 8 (a and b) shows the automatic spreading resistance (ASR) measurement of Pt top electrode covered PZT/SOI and PZT/Pt/SOI deposited at 400 °C and

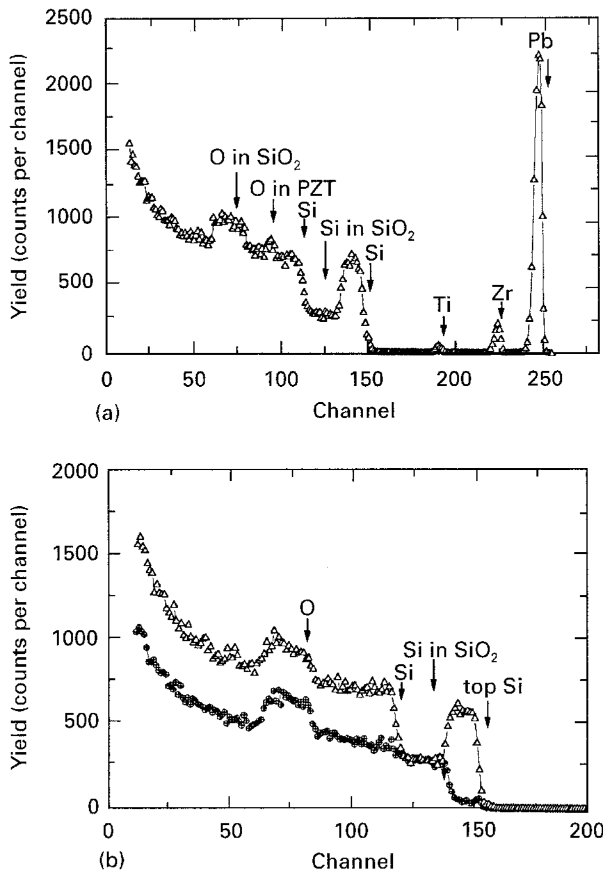

Figure 7 2 MeV He^+ RBS spectra from (a) PZT/SOI annealed at 650 °C for 120 s and (b) SOI substrate before PZT growth with simulation performed for a (⊕) aligned and (Δ) random system.

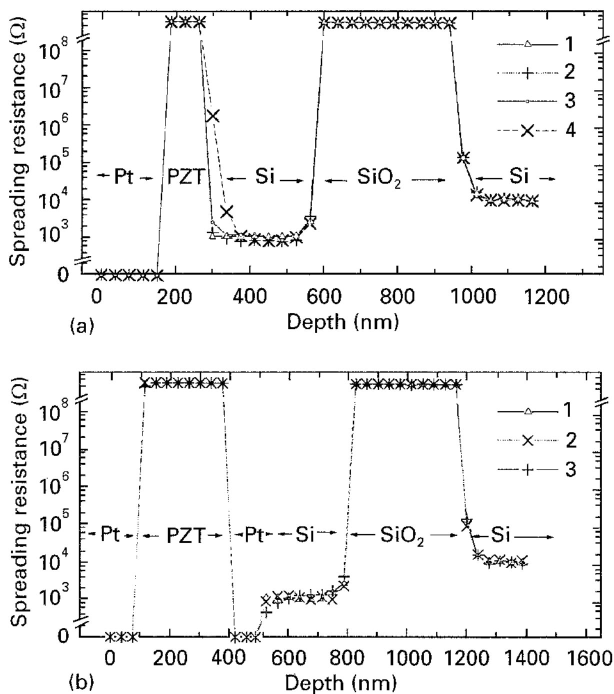

Figure 8 ASR measurement results of (a) Pt/PZT/SOI samples annealed at 650 °C for different time intervals and (b) Pt/PZT/Pt/SOI samples annealed at 650 °C for different time intervals (1: before PZT growth; 2: annealed for 3 min; 3: annealed for 7 min; 4: annealed for 30 min).

annealed at 650 °C. We see that the PZT layer as well as the SiO_2 layer were highly resistive ($10^{11}\ \Omega\cdot$cm), and that the interfaces between PZT and SOI as well as Pt/SOI were very abrupt electrically for short annealing times. However, we observed a clear semiconducting interface layer between PZT and SOI as the annealing time was increased to 30 min, which corresponds to interdiffusion between PZT and SOI. From Fig. 8, we also see that the electrical properties of SOI were not affected by the growth of the PZT layer, as is indicated by a comparison of ASR results taken both before and after growth.

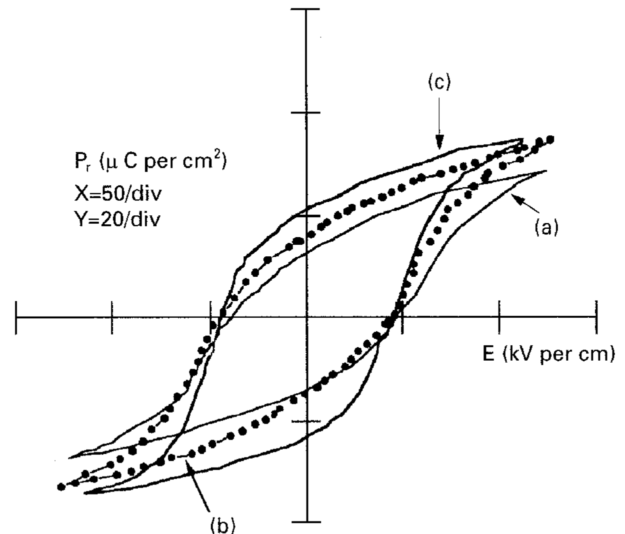

Figure 9 P–E hysteresis loop of PZT on Pt-coated SOI. (a) deposited at room temperature and annealed at 650 °C for 200 s, (b) deposited at 400 °C and annealed at 650 °C for 200 s, (c) deposited at 550 °C and annealed at 750 °C for 100 s.

The ferroelectric behaviour was investigated by measuring the P–E (polarization electric field) hysteresis loop using a modified Sawyer–Tower meter at a fixed 50 Hz frequency. The results are shown in Fig. 9 which indicate that the deposited films had good ferroelectric behaviour. However, films with a ⟨100⟩ preferred orientation show a slightly larger remanent polarization than that of a film with ⟨110⟩ preferred orientation.

4. Conclusions

Stoichiometric and well crystallized ferroelectric PZT thin films were grown on SOI and Pt-coated SOI by pulsed excimer laser deposition combined with RTA. The crystallographic structure of the films were found to be dependent on the annealing temperature and annealing time as well as the deposition temperature. Post-annealed films showed a ⟨100⟩ preferred orientation for relatively higher substrate temperature deposited samples and a ⟨110⟩ preferred orientation for the relatively lower temperature deposited films. The films grown on SOI were found to be more easily crystallized as compared to PZT films on bulk silicon due to the surface structure of the SOI. XTEM and RBS have shown that the interfaces between PZT and SOI as well as Pt-coated SOI can be controlled by RTA. The interfaces were very abrupt under the optimized annealing conditions and in addition the structure of the SOI was not affected by the PZT growth. ASR measurements have shown that the electrical properties at the interfaces of PZT/SOI and PZT/Pt/SOI were abrupt and also that the electrical properties

of the SOI were still good after the PZT growth. The experimental results show that laser deposition combined with rapid thermal annealing is an effective method to fabrication ferroelectric PZT films on SOI and Pt/SOI substrates.

References

1. G. C. MESSENGER and F. N. COPPAGE, *IEEE Tran. Nuclear.* **135** (1988) 1461.
2. J. F. SCOTT, C. A. ARAUJO, H. B. MEADOWS, L. D. McMILLAN and A. SHAWABKEH, *J. Appl. Phys.* **66** (1989) 1444.
3. K. IZUMI, *Vacuum* **42** (1991) 333.
4. C. E. D. CHEN, *Ibid.* **42** (1991) 383.
5. D. ROY and S. B. KRUPANIDHI, *J. Mater. Res.* **7** (1992) 2521.
6. S. K. DEY and R. ZULLEEG, *Ferroelectrics* **108** (1990) 47.
7. A. YAMANASHI, K. TANAKA, T. NAGATOMO and O. OMOTO. *Jpn. J. Appl. Phys.* **32** (1993) 4179.
8. K. J. REESON, K. G. STEPHENS and P. L. F. HEMMENT, *Nucl. Instrum. Methods Phys. Res.* **B37/38** (1989) 290.
9. LIRONG ZHENG, YIQING CHEN, CHENGLU LIN and SHICHANG ZOU, *Chin. Phys. Lett.* **11** (1994) 518.
10. LIRONG ZHENG, YIQING CHEN, CHENGLU LIN, WEIGEN LUO and SHICHANG ZOU, *Integ. Ferroelectrics* **9** (1995) 69.

Received 30 August 1995
and accepted 18 March 1996